http://dx.doi.org/10.5012/bkcs.2014.35.3.758

Vibrational Relaxation of Cyanate or Thiocyanate Bound to Ferric Heme Proteins Studied by Femtosecond Infrared Spectroscopy†

Seongchul Park, Jaeheung Park, Han-Wei Lin, and Manho Lim*

Department of Chemistry and Chemistry Institute for Functional Materials, Pusan National University, Busan 609-735, Korea
**E-mail: mhlim@pusan.ac.kr*
Received August 20, 2013, Accepted October 6, 2013

Femtosecond vibrational spectroscopy was used to measure the vibrational population relaxation time (T_1) of different anions bound to ferric myoglobin (Mb^{III}) and hemoglobin (Hb^{III}) in D_2O at 293 K. The T_1 values of the anti-symmetric stretching (ν_1) mode of NCS in the NCS^- bound to Mb^{III} ($Mb^{III}NCS$) and Hb^{III} ($Hb^{III}NCS$) in D_2O are 7.2 ± 0.2 and 6.6 ± 0.2 ps, respectively, which are smaller than that of free NCS^- in D_2O (18.3 ps). The T_1 values of the ν_1 mode of NCO in the NCO^- bound to Mb^{III} ($Mb^{III}NCO$) and Hb^{III} ($Hb^{III}NCO$) in D_2O are 2.4 ± 0.2 and 2.6 ± 0.2 ps, respectively, which are larger than that of free NCO^- in D_2O (1.9 ± 0.2 ps). The smaller T_1 values of the ν_1 mode of the heme-bound NCS suggest that intramolecular vibrational relaxation (VR) is the dominant relaxation pathway for the excess vibrational energy. On the other hand, the longer T_1 values of the ν_1 mode of the heme-bound NCO suggest that intermolecular VR is the dominant relaxation pathway for the excess vibrational energy in the ν_1 mode of NCO^- in D_2O, and that intramolecular VR becomes more important in the vibrational energy dissipation of the ν_1 mode of NCO in $Mb^{III}NCO$ and $Hb^{III}NCO$.

Key Words : Femtosecond vibrational spectroscopy, Intramolecular vibrational relaxation, Photophysical processes, Anion-bound heme proteins

Introduction

Heme proteins such as myoglobin (Mb) and hemoglobin (Hb) have been widely used as model systems for the study of protein dynamics and structure and their relation to its function.[1] Mb and Hb are oxygen storage and transport proteins, respectively, that contain a heme prosthetic group. These proteins reversibly bind small neutral ligands such as O_2, CO, and NO when the heme is in the ferrous form. Because the binding of ligand proceeds on the picosecond or nanosecond time scale, time-resolved spectroscopy has been used to probe the binding dynamics and structural changes induced by ligand binding after photodeligation of the ligand-bound proteins.[2-11] The quantum yield (QY) of photodeligation for these ligands in the ligated ferrous heme proteins by Soret or Q-band excitation in the visible region is significant,[2,12] and the photodeligation occurs on a subpicosecond time scale;[13,14] thus, ligated ferrous Mb (Mb^{II}) and Hb (Hb^{II}) have been ideal systems to study the ultrafast dynamics of ligand binding and conformational changes induced in the protein on ligand binding.[1] Various experimental and theoretical investigations have been carried out on ferrous hemes with small neutral ligands.[1-14]

Neutral ligands bind ferrous hemes, whereas anionic ligands bind ferric hemes.[15] Because ferric heme proteins are also known to participate in biological functions,[15,16] understanding the binding characteristics of ligands to both ferric and ferrous hemes is necessary to fully unveil the functioning mechanism of heme proteins. Compared to ferrous hemes, reports on the dynamics of ligand binding to ferric hemes are scarce.[16-18] According to recent studies on cyanide (CN^-) bound to ferric heme proteins such as Mb, Hb, and cytochrome *c*, CN^--bound heme proteins were photostable and did not undergo photodeligation.[16,18,19] Azide ion-bound Mb was also found to be photostable on photoexcitation.[17] Anion-bound heme proteins appear to be photostable, and thus the conventional method of investigation—probing ligand-binding dynamics after photodeligation of anion-bound ferric hemes—could not be utilized.

When a molecule is photoexcited, it either thermally and/or vibrationally relaxes after electronic relaxation or undergoes a photoreaction such as deligation. Time-resolved spectra have often been used to differentiate between photophysical and photochemical processes. However, if the transient spectra of the photophysical process are not well separated in time or frequency from those for the photochemical process, the two cannot be clearly distinguished. According to recent time-resolved IR (TRIR) spectra of photoexcited CN^--bound ferric Mb ($Mb^{III}CN$), a transient absorption, red-shifted by 30 cm^{-1} from the fundamental band, appeared immediately and decayed with a time constant of 3.6 ps. The values for the red shift and decay time constant are comparable with a typical anharmonicity and vibrational relaxation time (T_1) of a vibrationally excited heme ligand in the ground electronic state. Furthermore, 3.6 ps was too short to be the time constant for geminate rebinding (GR) of the ligand to the heme proteins. Therefore, the transient absorption in the TRIR spectrum was attributed to the vibrationally excited CN in $Mb^{III}CN$ instead of the deligated CN^-, and

†This paper is to commemorate Professor Myung Soo Kim's honourable retirement.

thus photodeligation was not accounted for. More recently, Champion and coworkers performed continuous-wave resonance Raman measurements on the photoexcited $Mb^{III}CN$ and concluded that $Mb^{III}CN$ undergoes photodeligation with a QY = 0.75, and that almost all the deligated CN^- geminately rebinds with a time constant of 3.6 ps.[20] They suggested that although the $Mb^{III}CN$ was being photodeligated, the extremely fast and highly efficient (99.99%) GR precluded the observation of the photodeligated state in time-resolved spectra.[20] Clearly, the characteristics of the vibrationally excited spectrum for ligands bound to heme proteins are critical to differentiate between the signals for photochemical processes from those for photophysical processes in the TRIR spectrum. Unfortunately, due to the weak extinction coefficient of the CN stretching mode, its T_1 value and anharmonicity were not directly measured in $Mb^{III}CN$. Other anions with reasonable extinction coefficients would be helpful in characterizing the photodynamics of anion-bound heme proteins after excitation by a visible pulse. NCO^- and NCS^- are good ligands for studying the dynamics of photoexcited anion-bound heme proteins because their extinction coefficients are large, their anti-symmetric stretching (ν_1) modes are located well away from the protein absorption, and their binding constants to heme are relatively large.

The vibrational relaxation (VR) rate and mechanism of energy transport for a molecule in solution are essential to understanding chemical reaction dynamics in condensed phases.[21] T_1 studies also provide important information regarding the structure and dynamics of solvated molecules.[21-23] For example, the T_1 of CO bound to heme proteins was measured to reveal the heme-ligand bond dynamics in CO-bound Mb^{II} ($Mb^{II}CO$) and Hb^{II} ($Hb^{II}CO$). The T_1 values of CO in $Mb^{II}CO$ and $Hb^{II}CO$ were found to be shorter than that in CO-bound protoheme, where the bound CO is not surrounded by a protein matrix but is instead exposed to solvent.[23] The T_1 of the CO bound to the heme was considerably shorter than the T_1 of metallocarbonyls (70–800 ps),[23-25] which was attributed to intramolecular VR (IVR) from CO to heme owing to the strong anharmonic coupling of the ligand and ring modes in the heme.[23,26,27] The VR times of NO bound to various hemes were also measured to explore its bonding dynamics in heme proteins and to properly assign its transient absorption signals in TRIR.[9,28,29] In contrast, the VR time of anions bound to ferric hemes is rarely investigated.

In this report, we characterized the vibrationally excited ν_1 modes of NCS and NCO anionic ligands bound to Mb^{III} and Hb^{III} using femtosecond IR pump-IR probe spectroscopy. Whereas T_1 was shortened in $Mb^{III}NCS$ and $Hb^{III}NCS$ compared to NCS^- dissolved in D_2O, it was lengthened in $Mb^{III}NCO$ and $Hb^{III}NCO$ compared to NCO^- dissolved in D_2O. The implication of the changes in the VR times of these anions bound to heme proteins is discussed.

Experimental

Femtosecond Infrared Spectrometer. A femtosecond infrared spectrometer used here was described previously.[8,29] Briefly, a home-built optical parametric amplifier, pumped by a commercial Ti:sapphire amplifier with a repetition rate of 1 kHz generating 110 fs pulses at 800 nm, was used to generate signal and idler pulses in the near IR region. The generated signal and idler pulses were mixed in an $AgGaS_2$ crystal for difference-frequency generation of a broad band (~130 cm^{-1}) mid-IR pulse with energy of about 1 μJ. A small portion of the intense IR pulse was reflected off a 2 mm thick BaF_2 wedged window for a probe pulse, and the transmitted beam was used as a pump pulse. The mutual polarization of the pump and probe pulses was set at the magic angle (54.7°) to obtain an isotropic absorption spectrum by rotating the polarization of the pump pulse by two IR polarizers. A chopper was used to block the pump beam at half the repetition rate to collect the pumped and unpumped absorption signals quasi-simultaneously.[8,29] The spectrally broad probe pulse passed through the sample and was routed to a 320 mm monochromator with a 150 *l*/mm grating equipped with a N_2(l)-cooled 64-element HgCdTe array detector. The spectral resolution of the probe pulse was approximately 1.54 cm^{-1}/pixel at 2100 cm^{-1}. The pump-induced change in the absorbance of the sample, ΔA, was obtained by subtracting the unpumped absorbance from the pumped one. The instrument response function was *ca.* 0.3 ps.

Sample Preparation. Lyophilized horse skeleton Mb^{III}, human Hb^{III}, NaOCN, NaSCN were purchased from Sigma-Aldrich Co. and used without further purification. Mb^{III} was dissolved in D_2O buffered with 0.1 M potassium phosphate (pD 7.4), and the solution was centrifuged to remove any aggregates and undissolved impurities. Concentrated NCO^- and NCS^- solutions were also prepared in the same phosphate D_2O buffer solution by dissolving the corresponding sodium salt. A small amount of anion solution was added to the filtered Mb^{III} solution to prepare anion-bound Mb^{III}. Because the binding constant of the anions to Mb^{III} is finite, the final solution is a mixture of ligated Mb^{III}, Mb^{III}, and free anion. The initial concentrations of Mb^{III} and anions in the mixture were 10 mM and 10–20 mM, respectively, meaning that 50–80% of the added Mb^{III} was ligated. $Hb^{III}NCO$ and $Hb^{III}NCS$ were prepared in the same way as the Mb^{III} adducts. Because Hb has four heme units, the heme concentration of Hb is four times that of the Hb concentration. For the sake of better comparison, the concentration of heme will be used in place of Hb concentration hereafter. As 10 mM of Hb^{III} and 10–20 mM of anions were mixed, the final solution also became a mixture of ligated Hb^{III}, Hb^{III}, and free anion, and 50–80% of the Hb^{III} was ligated. The NCO^- or NCS^--bound heme proteins was loaded in a gas-tight 27 μm or 130 μm path length sample cell with two CaF_2 windows, respectively. The sample cell was rotated sufficiently quickly so that each laser pulse excited a fresh volume of the sample. D_2O was used to avoid strong water absorption in the spectral region of interest. Because D_2O absorption is much lower near 2000 cm^{-1}, where the Fe(III)NCS adduct absorbs, than near 2160 cm^{-1}, where the Fe(III)NCO adduct absorbs, a

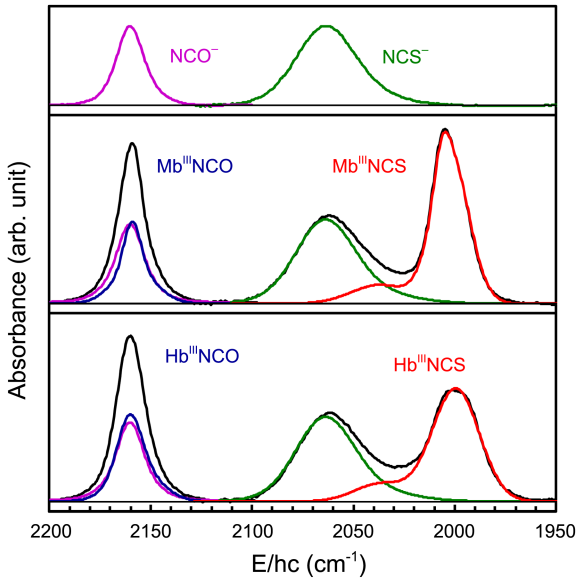

Figure 1. Equilibrium absorption spectra of the ν_1 mode of NCO^- (pink) and NCS^- (green) in D_2O buffer, NCO (blue) in $Mb^{III}NCO$ and $Hb^{III}NCO$, and NCS (red) in $Mb^{III}NCS$ and $Hb^{III}NCS$ at 293 K. The absorption band collected for mixtures of protein and anion was decomposed into the absorption bands for ligated protein and free anion. The absorbance is normalized to the peak intensity of NCO^- or NCS^- in D_2O.

longer path length was utilized for the Fe(III)NCS adduct. The integrity of the sample was checked by UV-Vis and FT-IR spectroscopy. The temperature of the entire lab was maintained at 293 ± 1 K.

Results and Discussion

Figure 1 shows the vibrational absorption bands of the ν_1 mode of NCS and NCO as ions in D_2O buffer solution and as ligands in $Mb^{III}NCO$, $Mb^{III}NCS$, $Hb^{III}NCO$, and $Hb^{III}NCS$ in the same buffer solution at 293 K. Due to the finite value of the binding constant, not all of the heme proteins in solution are ligated by the added anions. When 20 mM of NCO^- or 10 mM of NCS^- was mixed with 10 mM of heme, approximately 80% or 50% of the heme was ligated by the anion, respectively. Table 1 summarizes the experimentally determined spectral parameters for the ν_1 mode of NCO and NCS as free anions or ligated to Mb^{III} and Hb^{III} dissolved in D_2O buffer at 293 K, as well as the binding constants of the anions to the heme proteins. The T_1 values determined in this work are also shown in Table 1. The vibrational bands of the $Mb^{III}NCS$ and $Hb^{III}NCS$ solutions show two absorption features with one feature mimicking the absorption band of free NCS^- in solution. The absorption bands for $Mb^{III}NCS$ and $Hb^{III}NCS$ were obtained by carefully removing that of the free NCS^- in solution. As can be seen in Figure 1, the vibrational bands for $Mb^{III}NCS$ and $Hb^{III}NCS$ show two peaks, suggesting that there are two conformations in $Mb^{III}NCS$ and $Hb^{III}NCS$. Several vibrational bands, which were attributed to different conformations, were observed in the exogenous ligand-bound heme proteins.[2] The two vibrational bands were described by two Gaussian functions. The major band (85%) of $Mb^{III}NCS$ was centered at 2005 cm^{-1} with a full width at half maximum (FWHM) of 20 cm^{-1}, and the minor band (15%) appeared at 2037 cm^{-1} with a FWHM of 33 cm^{-1}. From the separated absorption intensity, the binding constants of NCS^- to the heme proteins were calculated: K_{MbNCS} = 126 and K_{HbNCS} = 160 at 293 K. The calculated binding constants are consistent with the reported values.[30] The relative intensities of the conformation bands of $Mb^{II}CO$ have been used to account for the populations of the corresponding conformations, which implies that the conformational bands have the same absorptivity.[2] Based on the assumption that the absorptivities of the two bands in $Mb^{III}NCS$ and $Hb^{III}NCS$ are the same, the integrated extinction coefficients of the ν_1 band of NCS in $Mb^{III}NCS$ and $Hb^{III}NCS$ were calculated to be 47 ± 3 and 37 ± 3 $mM^{-1}\cdot cm^{-1}$, respectively, almost twice that of free NCS^- in D_2O (21 ± 2 $mM^{-1}\cdot cm^{-1}$). In the case of $Mb^{III}NCO$ and $Hb^{III}NCO$ in solution, the absorption bands have only one feature that is very similar to the absorption band of NCO^- in D_2O, indicating that the ν_1 bands of NCO in $Mb^{III}NCO$ and $Hb^{III}NCO$ are almost the same as that of free NCO^- in D_2O buffer. The absorption bands of $Mb^{III}NCO$ and $Hb^{III}NCO$ in solution were obtained by carefully removing the absorption band of free NCO^- in D_2O, the contribution of which was calculated

Table 1. Spectral and dynamics parameters for the ν_1 mode of NCO and NCS as free anions or ligated to Mb^{III} and Hb^{III} dissolved in D_2O buffer (pD = 7.4) at 293 K. The binding constants of the anions to the ferric heme proteins are also tabulated

	Association constant	Center freq. (cm^{-1})	FWHM (cm^{-1})	Anharmonicity (cm^{-1})	Integrated band intensity ($mM^{-1}cm^{-1}$)	T_1 (ps)
NCO^-		2160.2	16.8	19	39	1.9 ± 0.2 ps
$Mb^{III}NCO$	460	2159	13	19	56	2.6 ± 0.2 ps
$Hb^{III}NCO$	450	2160	17	18	49	2.4 ± 0.2 ps
NCS^-		2064	36	23[b]	21	18.3 ps[b]
$Mb^{III}NCS$[a]	126	2005(85%)	20	24	47	7.2 ± 0.2 ps
		2037(15%)	33			
$Hb^{III}NCS$[a]	160	2000(85%)	27	22	37	6.6 ± 0.2 ps
		2036(15%)	31			

[a]The ν_1 mode of NCS in this compound has two absorption bands. The percent in the parentheses of the central frequency is the relative magnitude of the two bands. [b]These values are taken from a previous report.[21] Experimental values without error range are estimated to have 2–5% uncertainty.

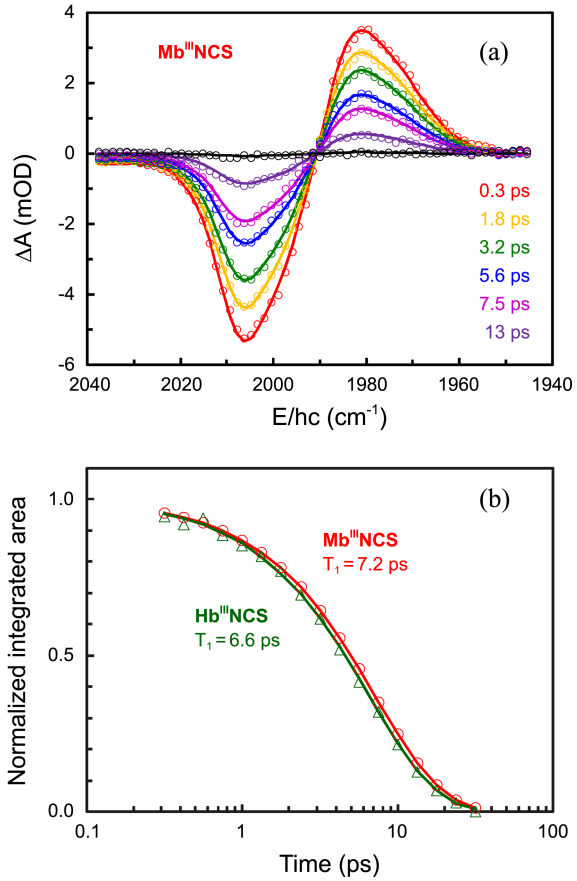

Figure 2. (a) Representative transient vibrational spectra of the ν_1 mode of NCS in Mb^{III}NCS in D_2O at 293 K after excitation by an intense IR pulse tuned to the fundamental band of the ν_1 mode. The negative feature (inverted fundamental band) arises from the population loss in the v = 0 state of the ν_1 mode due to photo-excitation, and the transient absorption (hot band) from the population gain in the v = 1 state. The hot band is red-shifted from the fundamental band by 24 cm^{-1}, the anharmonicity of the ν_1 mode of NCS in Mb^{III}NCS. (b) Normalized time-dependent integrated areas of ΔA in the ν_1 mode of NCS in Mb^{III}NCS (red open circles) and Hb^{III}NCS (green open triangles). The changes are well described by an exponential function with time constants of 7.2 (red line) and 6.6 ps (green line). The time constants represent the T_1 values of the ν_1 mode of NCS in the corresponding compounds.

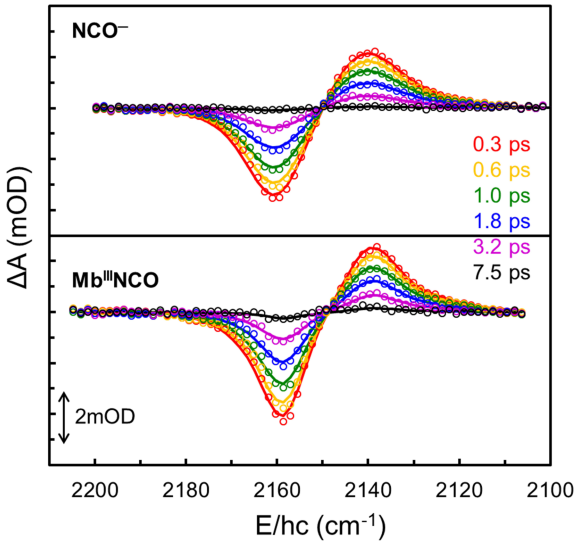

Figure 3. (a) Representative transient vibrational spectra of the ν_1 mode of NCO$^-$ in D_2O buffer (upper panel) and NCO in Mb^{III}NCO (lower panel). The data (open circles) were described by the time-dependent inverted fundamental band plus the hot band (solid line). The pump-probe time delays are 0.3, 0.6, 1.0, 1.8, 3.2, and 7.5 ps and are color-coded.

with the estimated binding constants for the samples: K_{MbNCO} = 460 and K_{HbNCO} = 450 at 273 K. The binding constants were estimated from the temperature dependence of the reported binding constants.[31] From the separated absorption intensities and the concentrations calculated from the binding constants, the integrated extinction coefficients of the ν_1 bands of NCO in Mb^{III}NCO and Hb^{III}NCO were calculated to be 56 ± 3 and 49 ± 3 mM^{-1}·cm^{-1}, respectively, approximately 1.3 times that of free NCO$^-$ in D_2O (39 ± 2 mM^{-1}·cm^{-1}). When ± 20% of the binding constant was used for the separation of the absorption band, the recovered absorption bands for Mb^{III}NCO and Hb^{III}NCO were within the uncertainty reported here.

Although 20–50% of the heme in the protein solution is not ligated by the added anion, the presence of the free protein does not affect the T_1 measurements of the ν_1 mode of the triatomic ligands because the IR pulse selectively excites the ligated protein as free protein does not absorb the IR pulse tuned to the absorption band of the ligand. In addition, the presence of the free anion in the solution can be delineated if the absorption band of the free anion is distinguished from that of bound anion. For the thiocyanate ion bound to the heme proteins, the ν_1 band of the anion bound to the heme proteins is red-shifted by 20–60 cm^{-1}, and the vibrational band of the bound anion is well separated from that of the free anion. Therefore, the ν_1 bands in Mb^{III}NCS and Hb^{III}NCS were selectively excited. Figure 2(a) shows the TRIR spectra of the ν_1 band of NCS in Mb^{III}NCS after excitation with an intense IR pulse. The bleach signal, mimicking the inverted equilibrium ν_1 band of NCS in Mb^{III}NCS, arises from the loss in the population of the ground vibrational state due to the excitation by an intense IR pulse tuned to the ν_1 mode. The transient absorption, red-shifted from the fundamental band by 24 cm^{-1} (the anharmonicity of the ν_1 band of NCS), arises from the gain in the population of the v = 1 state. The integrated areas of both bleach and absorption in the Mb^{III}NCS decay with the same time constant of 7.2 ± 0.2 ps (Figure 2(b)). Almost the same spectral behavior was observed in the TRIR spectra of Hb^{III}NCS, except a slightly faster decay of the transients with T_1 = 6.6 ± 0.2 ps. The T_1 values for Mb^{III}NCS and Hb^{III}NCS are much smaller than that of free NCS$^-$ in D_2O (18. 3 ps).[21]

The ν_1 band of free NCO$^-$ heavily overlaps with those of Mb^{III}NCO and Hb^{III}NCO. Therefore, the vibrationally excited spectra of Mb^{III}NCO solution contain contributions from both the ν_1 bands of Mb^{III}NCO and free NCO$^-$. The TRIR spectra of free NCO$^-$ and Mb^{III}NCO in solution are shown in

Figure 3. The transient spectra of free NCO^- show an instantaneous bleach of the fundamental band and an absorption band red-shifted by 19 cm^{-1} from the fundamental band (the anharmonicity of the ν_1 band of NCO^-). The integrated areas of both the bleach and the absorption of the transient decay with a time constant of 1.9 ± 0.2 ps, much shorter than the T_1 of 2.8 ps for NCO^- dissolved in methanol.[21] The TRIR spectra of $Mb^{III}NCO$ in solution in the ν_1 band region are slightly different from those of free NCO^-. Because $Mb^{III}NCO$ in solution is a mixture containing free heme and anion, the ν_1 bands of NCO in both $Mb^{III}NCO$ and free NCO^- contribute to the transient of $Mb^{III}NCO$ in solution. The transient spectra were separated for each contribution (Figure 4). The transient spectra were fitted, including the known contribution from the vibrationally excited free NCO^- at each delay time, and the decay of the ν_1 band of NCO in $Mb^{III}NCO$ was recovered. As shown in Figure 4, the free NCO^- contributes approximately 50% of the transient spectra at a pump-probe delay of 0.4 ps, and its contribution becomes smaller as the delay time increases, implying that the ν_1 mode of NCO in $Mb^{III}NCO$ decays more slowly. The integrated area of the ν_1 band of NCO in $Mb^{III}NCO$ decayed with a time constant of 2.6 ± 0.2 ps (Figure 5). When the contribution of the free anion was varied by ± 20% of the calculated value in fitting the transients, the recovered decay time was within the uncertainty given here. The T_1 value of the ν_1 band of NCO in $Hb^{III}NCO$, which was obtained in the same way as that in $Mb^{III}NCO$, was found to be 2.4 ± 0.2 ps (Figure 5).

In typical T_1 measurement experiments, the time-dependent absorption change at the peak of the bleach or absorption is probed.[23,32-36] When the absorption band to be probed is distinctly separate from the other absorption that can be influenced by the IR pump pulse, the decay kinetics at the peak absorption or bleach can be a good representation of the T_1 of the corresponding vibrational mode. The time constants for the decays of the peak absorptions in the transients of $Mb^{III}NCS$ and $Hb^{III}NCS$ were almost the same as their T_1 values. Because the absorptions of $Mb^{III}NCO$ and $Hb^{III}NCO$

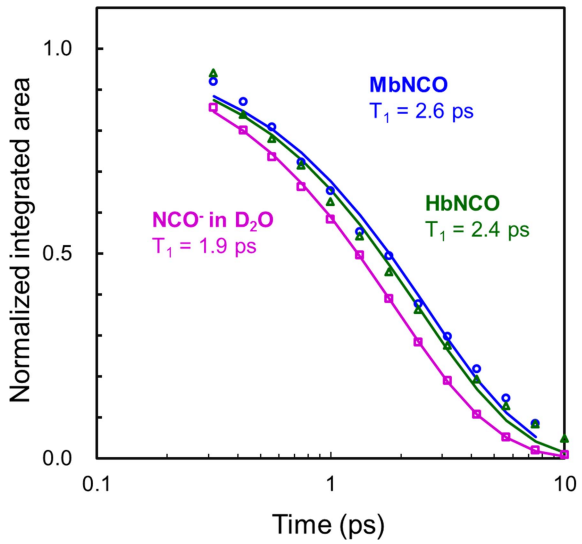

Figure 5. Normalized time-dependent integrated areas of ΔA in the ν_1 mode of NCO^- in D_2O buffer (pink open squares) and NCO in $Mb^{III}NCO$ (blue open circles) and $Hb^{III}NCO$ (green open triangles). The changes are well described by an exponential function with time constants of 1.9 (pink line), 2.6 (blue line), and 2.4 ps (green line). The time constants represent the T_1 values of the ν_1 mode of NCO in the corresponding compounds.

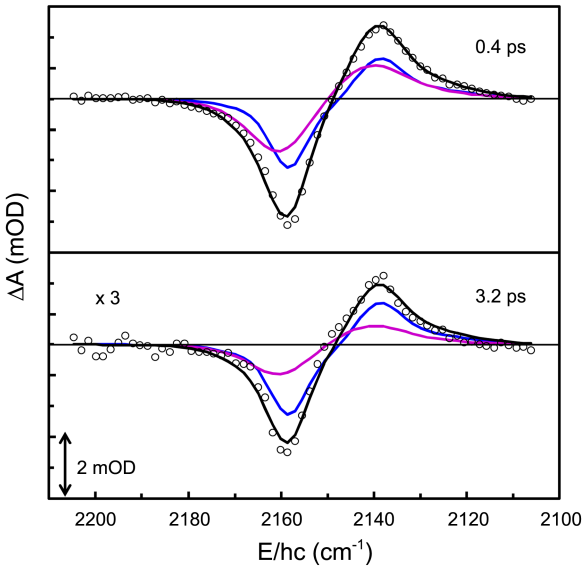

Figure 4. Transient vibrational spectra of $Mb^{III}NCO$ at pump-probe delays of 0.4 (upper panel) and 3.2 ps (lower panel). The transient spectra were decomposed into the ν_1 bands of NCO^- in D_2O buffer (pink line) and NCO in $Mb^{III}NCO$ (blue line). The sum of the two components (black line) describes the data well (open circles). The transient signal in the lower panel is 3 × magnified for a better view.

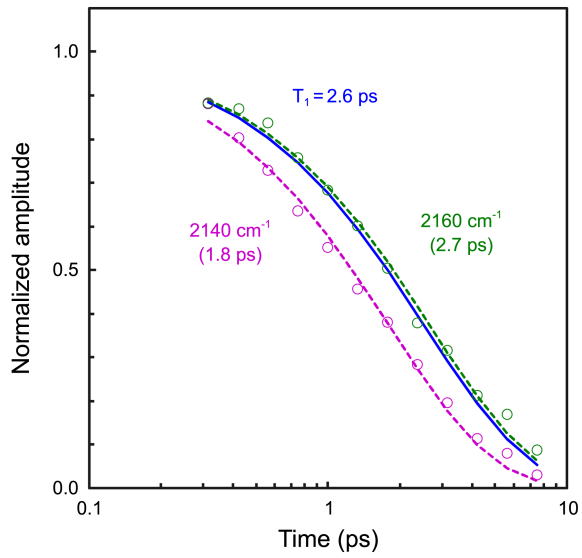

Figure 6. Normalized change of the peak absorption at 2140 cm^{-1} (pink open circles) and peak bleach at 2160 cm^{-1} (green open circles) in the TRIR spectra of the ν_1 mode of NCO in $Mb^{III}NCO$. For comparison, the decay with a time constant of 2.6 ps, the T_1 of the ν_1 band, is also shown (blue line). The peak amplitudes decayed with time constants of 1.8 (pink dashed line) and 2.7 ps (green dashed line).

heavily overlap with that of the free anion, the decays at the peak absorptions cannot be used to determine their T_1 values. Figure 6 compares the decay kinetics of the peak absorption and bleach in the TRIR spectra of $Mb^{III}NCO$ solution with the decay with T_1 value obtained in our analysis. The time constants vary depending heavily on the peak position probed. The discrepancy depends on the degree to which the absorption of the free anion contributes to the overall absorption. Clearly, probing whole TRIR spectra and their careful analysis is necessary to accurately determine the T_1 of a band that is heavily overlapped with another species, as it cannot be measured by probing the kinetics at a single wavelength.

The ν_1 mode of NCS^- is localized as a CN stretching motion.[34] Tominaga and coworkers investigated the T_1 values of the ν_1 mode of NCS^- in various polar solvents and found that T_1 was more than twice as long in aprotic solvents.[35] Similar behavior was also observed in the CN stretching mode of cyanide-bound metal complexes.[36] The faster VR in protic solvents was attributed to hydrogen bonding between the anion and solvent.[36] It was suggested that VR to the solvent vibrational modes, called external VR (EVR), contributes more than VR to the other vibrational modes of the anion (IVR), in the energy dissipation of the excited ν_1 mode of NCS in solvated NCS^-.[35] The strong hydrogen bonding plays an important role in the EVR process. The T_1 values of the ν_1 mode of NCS in $Mb^{III}NCS$ and $Hb^{III}NCS$ are *ca.* 3 times smaller than that of free NCS^- in D_2O, where stronger hydrogen bonding between the anion and the solvent exists. The faster VR in the ligand bound to heme indicates that IVR in $Mb^{III}NCS$ and $Hb^{III}NCS$ is more efficient. Because heme has many vibrational modes that can anharmonically couple to the ν_1 mode of NCS, the faster VR in $Mb^{III}NCS$ and $Hb^{III}NCS$ can be attributed to the efficient IVR process. Evidently, VR of the ν_1 mode of NCS in $Mb^{III}NCS$ and $Hb^{III}NCS$ is dominated by IVR to the heme vibrational modes.

VR of the ν_1 mode of NCO^- in D_2O is > 10 times more efficient than that of NCS^- in D_2O. The slower VR of NCS^- was attributed to its more localized normal coordinate and different charge distribution.[21] As mentioned, D_2O has a 2.4 times stronger absorption at 2160 cm^{-1}, where the ν_1 mode of NCO^- absorbs, than at 2060 cm^{-1}, where the ν_1 mode of NCS^- absorbs. Because the VR of a solute can be facilitated by a higher density of states in the solvent overlapping with the vibrational mode of the solute that is strongly hydrogen bonded to the solvent, the faster VR of NCO^- likely arises from the efficient EVR of the ν_1 mode to D_2O. The slower VR of the ν_1 mode in $Mb^{III}NCO$ and $Hb^{III}NCO$ implies that its EVR process is not as efficient as that of free NCO^- in D_2O. Since the NCO moiety is surrounded by a protein matrix, it is likely to experience weaker hydrogen bonding than free NCO^- in D_2O. Although the cyanate bound to heme has a slower VR than free NCO^- in D_2O, it still has faster VR than thiocyanate bound to heme, suggesting that the IVR process in the Fe(III)NCO adduct is more efficient than that in the Fe(III)NCS adduct. Many overtone and combination modes of heme vibrational modes were thought to be resonant with the high frequency modes of the exogenous ligand, thereby serving as a bath to accept the excess energy in the ligand.[37]

In addition to gaining insight on the VR of polyatomic systems, as mentioned before, VR time and anharmonicity of the vibrationally excited spectrum for ligands bound to heme proteins are very useful in isolating photophysical processes in the TRIR spectrum obtained after visible excitation. In other words, the characteristics of the vibrationally excited spectrum can be utilized in extracting photochemical processes in cyanate or thiocyanate bound to ferric heme proteins, which may be used to clarify the photostability of anion bound heme proteins.

Conclusion

We measured T_1 values for the ν_1 bands of NCO in $Mb^{III}NCO$ and $Hb^{III}NCO$ and NCS in $Mb^{III}NCS$ and $Hb^{III}NCS$ at 293 K. The ν_1 mode of $Mb^{III}NCS$ or $Hb^{III}NCS$ in D_2O has two bands near 2000 and 2040 cm^{-1}, red-shifted from the band of free NCS^- in D_2O at 2064 cm^{-1}. In contrast, the ν_1 mode of $Mb^{III}NCO$ or $Hb^{III}NCO$ in D_2O shows one band near 2160 cm^{-1}, which is at almost the same location as the band of free NCO^- in D_2O, suggesting that the bonding characteristics of NCO^- changed very little upon binding to the ferric heme proteins. Because the ν_1 bands of NCO in $Mb^{III}NCO$ and $Hb^{III}NCO$ heavily overlap with that of free NCO^- in D_2O, their T_1 values were obtained by carefully removing the contribution of the free NCO^- to the TRIR spectra of the corresponding protein solutions. The T_1 values for the ν_1 bands of $Mb^{III}NCO$ and $Hb^{III}NCO$ are 2.6 ± 0.2 and 2.4 ± 0.2 ps, respectively, and are larger than that of free NCO^- in D_2O buffer (T_1 = 1.9 ± 0.2 ps). The T_1 values for the ν_1 bands of $Mb^{III}NCS$ and $Hb^{III}NCS$ are 6.6 ± 0.2 and 7.2 ± 0.2 ps, respectively, and are smaller than that of free NCS^- in D_2O buffer (T_1 = 18.3 ps). The VR of the ν_1 mode of cyanate or thiocyanate bound to Mb^{III} and Hb^{III} appears to be dominated by IVR to the heme vibrational modes. Faster VR in the ν_1 mode of NCO than NCS in the corresponding heme ligands suggests that intramolecular VR is more efficient in the NCO ligand than in the NCS ligand.

Acknowledgments. This work was supported by a 2-Year Research Grant of Pusan National University.

References

1. Springer, B. A.; Sligar, S. G.; Olson, J. S.; Phillips, G. N., Jr. *Chem. Rev.* **1994**, *94*, 699-714.
2. Ansari, A.; Berendzen, J.; Braunstein, D. K.; Cowen, B. R.; Frauenfelder, H.; Hong, M. K.; Iben, I. E. T.; Johnson, J. B.; Ormos, P.; Sauke, T. B.; Scholl, R.; Schulte, A.; Steinbach, P. J.; Vittitow, J.; Young, R. D. *Biophys. Chem.* **1987**, *26*, 337-355.
3. Austin, R. H.; Beeson, K. W.; Eisenstein, L.; Frauenfelder, H.; Gunsalus, I. C. *Biochemistry* **1975**, *14*, 5355-5373.
4. Chernoff, D. A.; Hochstrasser, R. M.; Steele, W. A. *Proc. Natl. Acad. Sci. USA.* **1980**, *77*, 5606-5610.

5. Cornelius, P. A.; Hochstrasser, R. M.; Steele, A. W. *J. Mol. Biol.* **1983**, *163*, 119-128.
6. Henry, E. R.; Sommer, J. H.; Hofrichter, J.; Eaton, W. A. *J. Mol. Biol.* **1983**, *166*, 443-451.
7. Kim, J.; Park, J.; Lee, T.; Lim, M. *J. Phys. Chem. B* **2012**, *116*, 13663-13671.
8. Kim, S.; Jin, G.; Lim, M. *J. Phys. Chem. B* **2004**, *108*, 20366-20375.
9. Kim, S.; Park, J.; Lee, T.; Lim, M. *J. Phys. Chem. B* **2012**, *116*, 6346-6355.
10. Petrich, J. W.; Lambry, J. C.; Kuczera, K.; Karplus, M.; Poyart, C.; Martin, J. L. *Biochemistry* **1991**, *30*, 3975-3987.
11. Szabo, A. *Proc. Natl. Acad. Sci. USA.* **1978**, *75*, 2108-2111.
12. Ye, X.; Demidov, A.; Champion, P. M. *J. Am. Chem. Soc.* **2002**, *124*, 5914-5924.
13. Petrich, J. W.; Poyart, C.; Martin, J. L. *Biochemistry* **1988**, *27*, 4049-4060.
14. Anfinrud, P. A.; Han, C.; Hochstrasser, R. M. *Proc. Natl. Acad. Sci. USA.* **1989**, *86*, 8387-8391.
15. Antonini, E.; Brunori, M. *Hemoglobin and Myoglobin in their Reactions with Ligands (Frontiers of Biology, Vol. 21)*; North-Holland, 1971.
16. Helbing, J.; Bonacina, L.; Pietri, R.; Bredenbeck, J.; Hamm, P.; van Mourik, F.; Chaussard, F. i.; Gonzalez-Gonzalez, A.; Chergui, M.; Ramos-Alvarez, C.; Ruiz, C.; Lopez-Garriga, J. *Biophys. J.* **2004**, *87*, 1881-1891.
17. Helbing, J. *Chem. Phys.* **2012**, *396*, 17-22.
18. Kim, J.; Park, J.; Chowdhury, S. A.; Lim, M. *Bull. Korean Chem. Soc.* **2010**, *31*, 3771-3776.
19. Gruia, F.; Kubo, M.; Ye, X.; Champion, P. M. *Biophys. J.* **2008**, *94*, 2252-2268.
20. Zeng, W.; Sun, Y.; Benabbas, A.; Champion, P. M. *J. Phys. Chem. B* **2013**, *117*, 4042-4049.
21. Li, M.; Owrutsky, J.; Sarisky, M.; Culver, J. P.; Yodh, A.; Hochstrasser, R. M. *J. Chem. Phys.* **1993**, *98*, 5499-5507.
22. Dlott, D. D.; Fayer, M. D.; Hill, J. R.; Rella, C. W.; Suslick, K. S.; Ziegler, C. J. *J. Am. Chem. Soc.* **1996**, *118*, 7853-7854.
23. Owrutsky, J. C.; Li, M.; Locke, B.; Hochstrasser, R. M. *J. Phys. Chem.* **1995**, *99*, 4842-4846.
24. Heilweil, E. J.; Casassa, M. P.; Cavanagh, R. R.; Stephenson, J. C. *Annu. Rev. Phys. Chem.* **1989**, *40*, 143-171.
25. Shizuka, H.; Machii, M.; Higaki, Y.; Tanaka, M.; Tanaka, I. *J. Phys. Chem.* **1985**, *89*, 320-326.
26. Hill, J. R.; Dlott, D. D.; Rella, C. W.; Peterson, K. A.; Decatur, S. M.; Boxer, S. G.; Fayer, M. D. *J. Phys. Chem.* **1996**, *100*, 12100-12107.
27. Hill, J. R.; Ziegler, C. J.; Suslick, K. S.; Dlott, D. D.; Rella, C. W.; Fayer, M. D. *J. Phys. Chem.* **1996**, *100*, 18023-18032.
28. Park, J.; Lee, T.; Lim, M. *Chem. Phys.* **2013**, *442*, 107-114.
29. Park, J.; Lee, T.; Park, J.; Lim, M. *J. Phys. Chem. B* **2013**, *117*, 2850-2863.
30. Perry, C. B.; Chick, T.; Ntlokwana, A.; Davies, G.; Marques, H. M. *J. Chem. Soc., Dalton Trans.* **2002**, 449-457.
31. Jain, A.; Kassner, R. J. *J. Biol. Chem.* **1984**, *259*, 10309-10314.
32. Dahl, K.; Sando, G. M.; Fox, D. M.; Sutto, T. E.; Owrutsky, J. C. *J. Chem. Phys.* **2005**, *123*, 084504/084501-084504/084511.
33. Hill, J. R.; Tokmakoff, A.; Peterson, K. A.; Sauter, B.; Zimdars, D.; Dlott, D. D.; Fayer, M. D. *J. Phys. Chem.* **1994**, *98*, 11213-11219.
34. Ohta, K.; Maekawa, H.; Saito, S.; Tominaga, K. *J. Phys. Chem. A* **2003**, *107*, 5643-5649.
35. Ohta, K.; Tominaga, K. *Chem. Phys. Lett.* **2006**, *429*, 136-140.
36. Sando, G. M.; Zhong, Q.; Owrutsky, J. C. *J. Chem. Phys.* **2004**, *121*, 2158-2168.
37. Levy, D. H. *Annu. Rev. Phys. Chem.* **1980**, *31*, 197-225.